

See discussions, stats, and author profiles for this publication at: <https://www.researchgate.net/publication/240600790>

Heat Input and Temperature Distribution in Friction Stir Welding

Article in *Journal of Materials Processing and Manufacturing Science* · October 1998

DOI: 10.1106/55TF-PF2G-JBH2-1Q2B

CITATIONS

311

READS

9,817

5 authors, including:



W. Tang

University of South Carolina

21 PUBLICATIONS 2,123 CITATIONS

[SEE PROFILE](#)



John McClure

University of Texas at El Paso

82 PUBLICATIONS 4,563 CITATIONS

[SEE PROFILE](#)



Lawrence Murr

University of Texas at El Paso

780 PUBLICATIONS 26,507 CITATIONS

[SEE PROFILE](#)

Some of the authors of this publication are also working on these related projects:



AWS FRICTION STIR WELDING [View project](#)



3D printing/additive manufacturing; implant studies/trials [View project](#)

MIT Libraries Document Services/ Interlibrary Loan



ILLiad TN: 214281

ILL Number: 71600418



Yes No Cond

Borrower: SUC

In Process: 20101129

Lending String: *MYG,JHE,JHE,LHL,WTU

Patron: Upadhyay, Piyush; Graduate

Journal Title: Journal of materials processing & manufacturing science.

Volume: Issue:
Month/Year: 1998
Pages: 163-172

Article Author:

Article Title: W. Tang, X. Guo, J.C. McClure, L.E. Murr, A. Nunes; Heat Input and Temperature Distribution in Friction Stir Welding

Borrowing Notes:

OCLC# 25517123

Imprint: Lancaster, Pa. ; Technomic Pub. Co., c19

Shipping Method: Ariel

Call #: LSA no call#

Charge:

MaxCost: 30.00IFM

Library Address:
Document Services
Thomas Cooper Library
1322 Greene Street
University of South Carolina

Shipping Address:

Fax: 803 777-9503

Email Address: uscill@gwm.sc.edu

Request Type: Article
Document Type:

resending do not
bill again

2

Ariel Address: 129.252.80.49



US Copyright Notice

The copyright law of the United States (Title 17, United States Code) governs the making of reproductions of copyrighted material. Under certain conditions specified in the law, libraries are authorized to furnish a reproduction. One of these specified conditions is that the reproduction is not to be "used for any purpose other than private study, scholarship, or research." If a user makes a request for, or later uses, a reproduction for purposes in excess of "fair use," that user may be liable for copyright infringement. This institution reserves the right to refuse to accept a copying order if, in its judgment, fulfillment of the order would involve violation of Copyright Law.

Heat Input and Temperature Distribution in Friction Stir Welding

W. TANG, X. GUO, J. C. McCLURE¹ and L. E. MURR
Metallurgical and Materials Engineering Department
University of Texas at El Paso
El Paso, TX 79968 USA

A. NUNES
NASA
Marshall Space Flight Center
Huntsville, Alabama USA

Abstract: In this paper the heat input and temperature distribution during friction stir welding is investigated. The temperatures at different positions in the specimen thickness direction and perpendicular to the pin tool travel direction were recorded during welding under various welding conditions. It was found that the highest temperature in the welding seam is less than $0.8T_m$. For the conditions used in this work, the temperature does not change appreciably in the specimen thickness direction. The temperature distribution perpendicular to the weld is nearly isothermal under the pin tool shoulder. Furthermore, increasing welding pressure and pin tool rotational speed increases the peak welding temperature. Finally, it is shown that the shoulder of the pin tool plays a very important role in the welding process.

INTRODUCTION

ALUMINUM is usually welded by fusion methods such as TIG and plasma welding. The main difficulties when fusion welding methods are applied to aluminum alloys are, first, the adherent refractory aluminum oxide film, which is sometimes not removed completely and is entrained in the weld pool during the welding process, and second hot cracking and porosity that takes place during the melting and solidification process. Welding methods and parameters must be chosen very carefully to avoid these defects. Special methods such as variable polarity plasma and careful shielding must be used to break the aluminum oxide film and prevent new oxide film growth.

Friction stir welding is a newly developed solid state welding method [1]. Solid state welding (as opposed to fusion welding) methods are widely used in industry to avoid welding defects which always occur when molten metal solidifies, or to weld materials with a very high melting temperature. Traditional friction welding is usually performed on small axisymmetric parts, which can be rotated and pushed against each other to form a joint [2]. Friction stir welding on the other hand can be applied to various types of joints like butt joints, lap joints, T butt joints, and fillet joints [3]. In friction stir welding, the melting and solidification process does not occur, so there will be no shrinkage or hot cracking. Shielding gas is not needed since temperature is low. Other advantages of friction stir welding are presented elsewhere [3,4]. Previous work on friction stir welding has discussed the method itself and the microstructure of the welded joint [5–8], but the heat input and temperature distribution in the friction stir welded joints have never been presented before. This paper reports temperature isotherms and shows the effect of increasing pin tool pressure and rotational speed on the temperature distribution.

¹ Author to whom correspondence should be addressed.

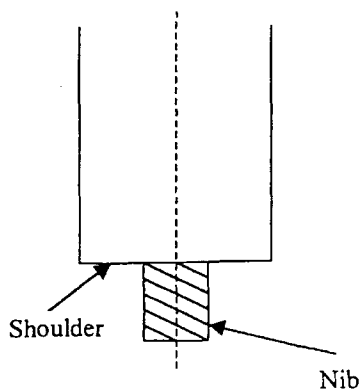


Figure 1. Schematic of pin tool.

WELDING PROCESS AND WELDING PARAMETERS

Experiments were performed on 6061 T6 aluminum. Most welds were bead on plate to permit temperature measurement on the centerline of the weld. The specimen size was 12 inches (304 mm) by 4 inches (101 mm) and 0.25 inches (6.4 mm) thick. Welds were made on Gorton Mastermil milling machine. The pin tool was made up of a screw nib and a shoulder made of tool steel as shown in Figure 1.

During the welding process, the aluminum plate was clamped against the work table with a steel backup plate, the rotational speed of the pin tool ranged from 300 rpm to 1200 rpm, and the travel speed was 2 mm/s. The downward pressure between the shoulder and the workpiece was controlled manually by raising the work table, to which the welded specimen is clamped, against the pin tool and judging the amount of material forced up at the edge of weld during welding. As a check on the consistency of the pressure used, the thickness variations of twenty random specimens were measured and found to be nearly equal to the thickness variations in the original plates. At the start of the weld, the average reduction of the thickness was about 3%.

TEMPERATURE MEASUREMENT

Temperatures during the friction stir welding process were measured by 30 gauge type K thermocouples imbedded in a series of small holes (0.92 mm diameter) at different distances from the weld seam drilled into the back surface of the workpiece. The holes were 4 inches from the start of the weld to allow equilibrium to develop. It was found that the existence of these holes does not affect the temperature field during the welding process [9]. Three depths of holes (1.59 mm, 3.18 mm and 4.76 mm) are used to measure the temperature field at one quarter, one half, and three quarters of the plate thickness. The thermocouples were inserted and secured to the bottom of the hole from the back side of the specimen. Thermally conducting paste was packed in the holes to seat the thermocouples. The temperature was recorded digitally using a National Instruments SCXI-1000 amplifier and Labview. Temperatures were sampled at 60 Hz so that several samples were taken per revolution of the nib. Digital signal smoothing was used as necessary to remove noise.

RESULTS AND DISCUSSION

Weld Temperature History

A cross section of a friction stir weld is shown in Figure 2 and a typical welding temperature history at different positions from the weld center is shown in Figure 3. It is seen that the welding temperature, including the peak temperature at the weld center, which is about 450°C, is below the melting temperature of the 6061 aluminum, which is 582°C [10]. The specimen after welding

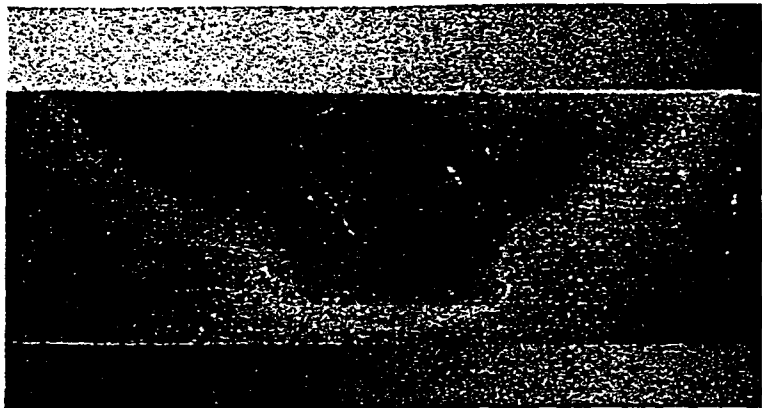


Figure 2. Cross section of typical weld. Workpiece is .25 in. thick.

shows that the weld center thermocouple was not destroyed by the pin tool but did change position slightly due to workpiece plastic flow. Microstructures of the welded joint also showed that there was no melting during the welding process. As expected, the friction stir welding process is a solid state welding process, and welding defects such as porosity and hot cracking are avoided. At the same time, with the stir and deformation process, the grain size of the welded zone is notably smaller and more equiaxed than that of the parent aluminum as a result of dynamic recrystallization [5,7,8].

Figures 4(a) and 4(b) show for comparison the original workpiece grain structures in contrast to the recrystallized grain structure in the weld center, respectively as observed by optical metallography. Figures 4(c) and 4(d) show these corresponding microstructures as observed in the transmission electron microscope. The initial workpiece microstructure [Figure 4(c)] is characterized by dense dislocation cells and tangles while the recrystallized grains within the weld zone [Figure 4(d)] contain a considerably reduced dislocation density and distributed precipitation similar to the original material. In addition, Murr et al. [8] have previously shown a wide variation in precipitation phenomena near the edges of the weld zone (Figure 2) and within a transition region which extends from about 8 to 15 mm on either side of the weld center line. This variation includes Guinier-Preston-like precipitates at the furthest distance, Widmanstätten ar-

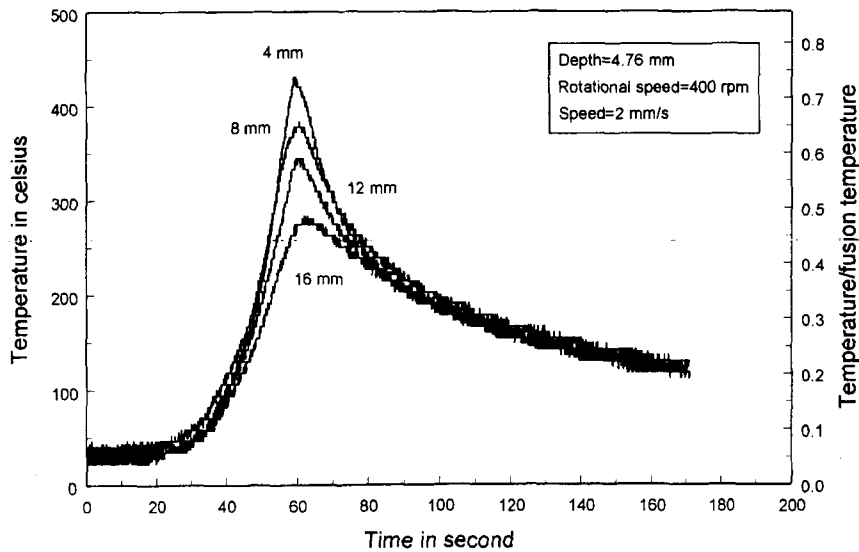


Figure 3. Typical temperature-time data for a weld made at 400 rpm and 2 mm/sec travel speed. Curves represent the temperature history at different distances from weld centerline.

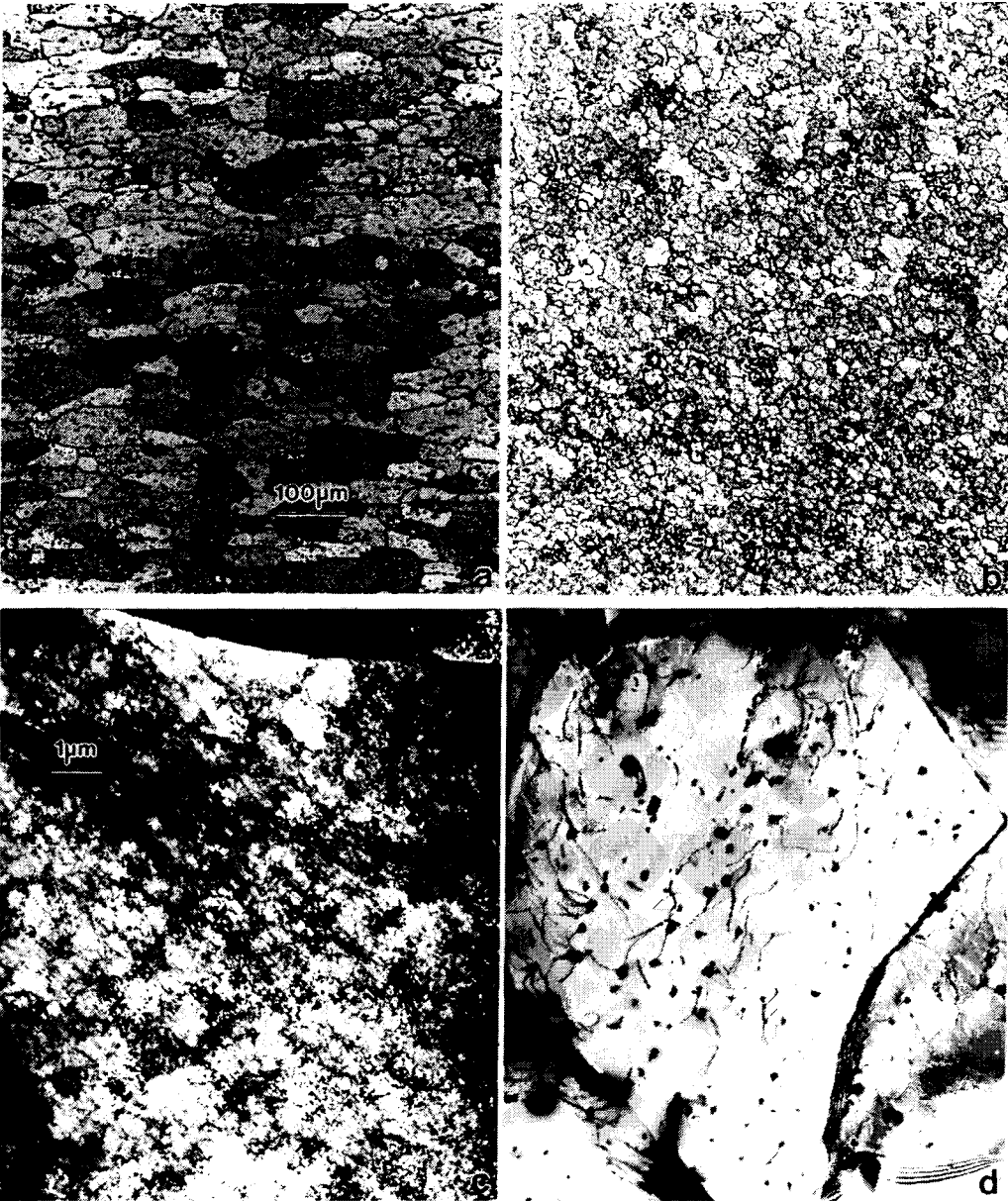


Figure 4. Comparison of initial 6061-T6 aluminum workpiece and weld zone microstructures. (a) Initial grain structure observed by light metallography. (b) Typical weld zone grain structure observed by light microscopy. (c) TEM image showing dislocation structure in (a). (d) TEM image showing corresponding microstructure in (b). Note homogeneously distributed precipitates. Magnifications in (a) and (b) are same. Magnifications in (c) and (d) are same.

rays of plate-like precipitates, and the more homogeneous precipitate particles in the weld zone are shown in Figure 4(d). These variations in precipitation microstructures were attributed to temperature variations or temperature field distributions. In this case, when the temperature increases and decreases continuously, the homogeneous precipitate, Widmanstätten arrays of plate-like precipitates, and the Guinier-Preston-like precipitates occur in regions where the peak temperatures were 450°C, 398°C, and 363°C, respectively.

TEMPERATURE FIELD DISTRIBUTION

From the temperature recorded during the welding process, the welding temperature distribution at different points away from the welding centerline and welding top surface could be determined. The peak temperature distribution at 400 rpm rotational speed is shown in Figure 5 for different depths below the top surface of the workpiece. The region near the nib is nearly isothermal suggesting that plastic deformation occurs away from the nib. From Figure 5 it is clear that the peak temperature gradient in the thickness direction of the welded joint is not large, and the fact that the grain sizes throughout the weld zone do not change appreciably from those shown in Figure 4(b) supports this conclusion. Welds made with a smaller shoulder radius to workpiece thickness ratio may show some gradient, however. Lower thermal conductivity materials than aluminum may also show some gradient.

A contraction of the isotherms with depth can be seen in Figure 6 due to the heat sinking of the backup plate below the workpiece and due to the greater distance from the shoulder/workpiece interface where considerable frictional heating takes place.

Thermocouples placed at equal distances from the weld seam but on opposite sides of the weld showed no differences in temperature. This would be expected since the total relative velocity of the nib and aluminum (one side is turning in the direction of workpiece motion and the other side is moving against it) is large compared to the difference in velocity on the two sides of the nib. Peak temperatures on both sides of the weld are shown in Figure 7.

INFLUENCE OF PRESSURE ON THE TEMPERATURE FIELD

As mentioned above, the welding pressure of the pin tool on the welded joint was controlled

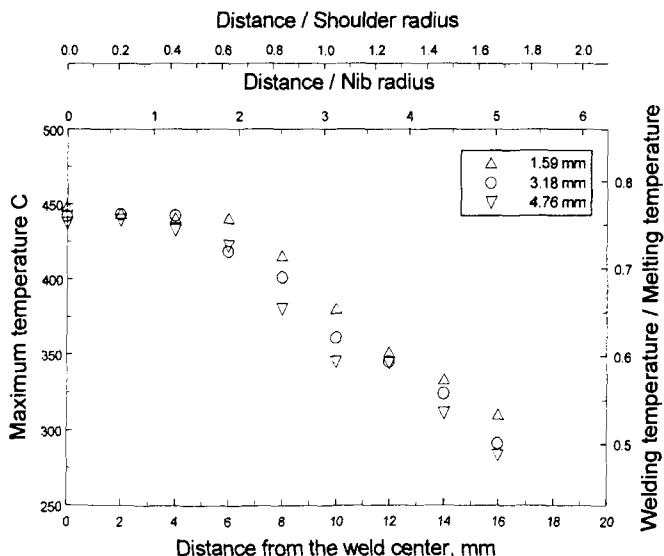


Figure 5. Maximum temperature as a function distance from weld seam. Data from three different depths in the sample is shown.

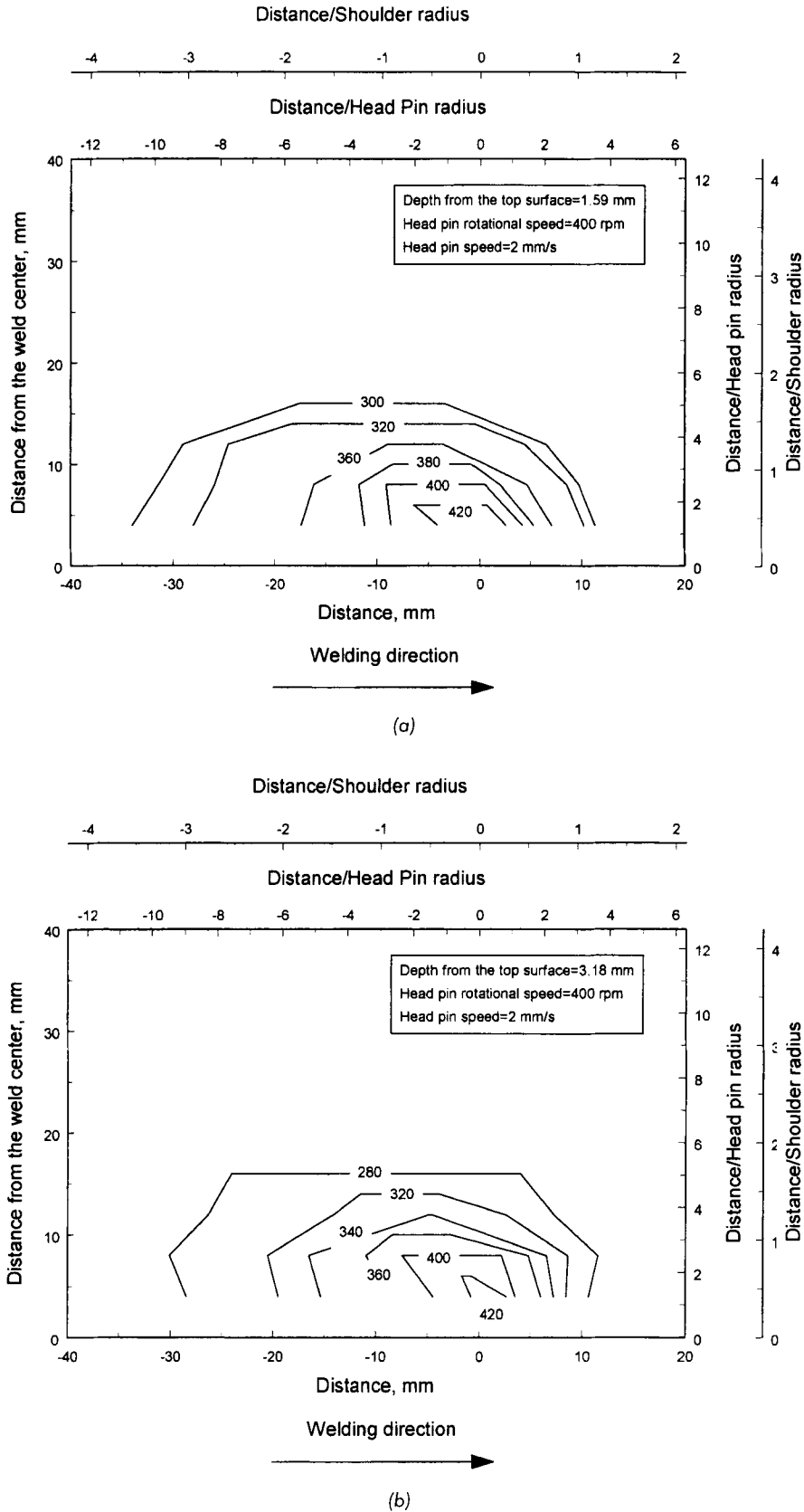


Figure 6. Isotherms at different depths below the workpiece surface: (a) depth = 1.6 mm, (b) depth = 3.2 mm and (c) depth = 4.8 mm.

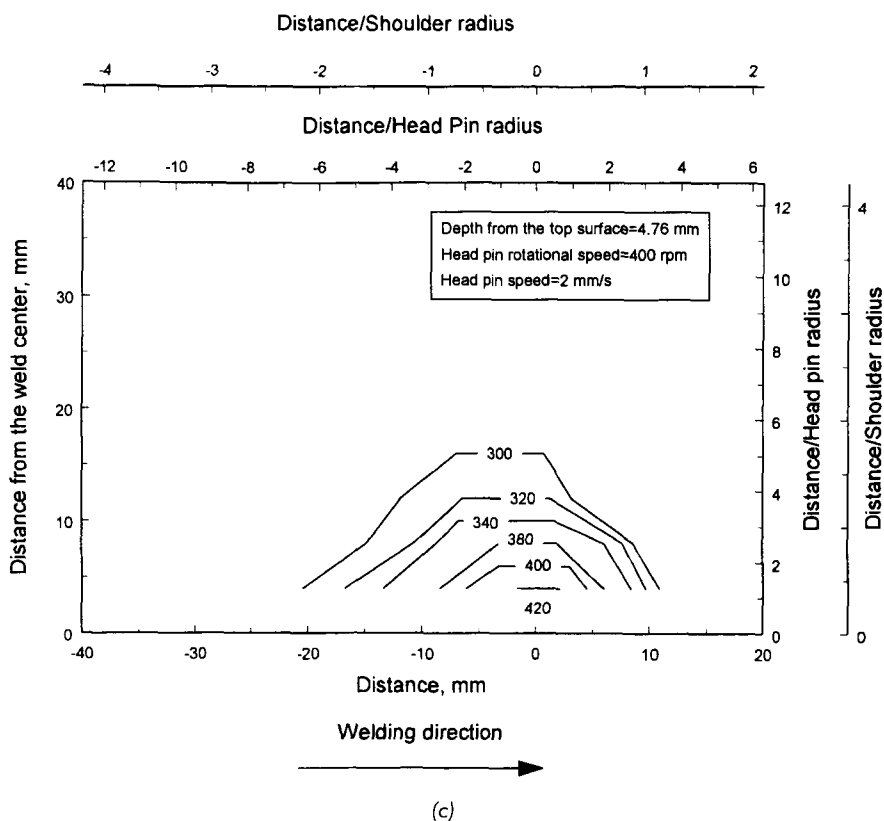


Figure 6 (continued). Isotherms at different depths below the workpiece surface: (a) depth = 1.6 mm, (b) depth = 3.2 mm and (c) depth = 4.8 mm.

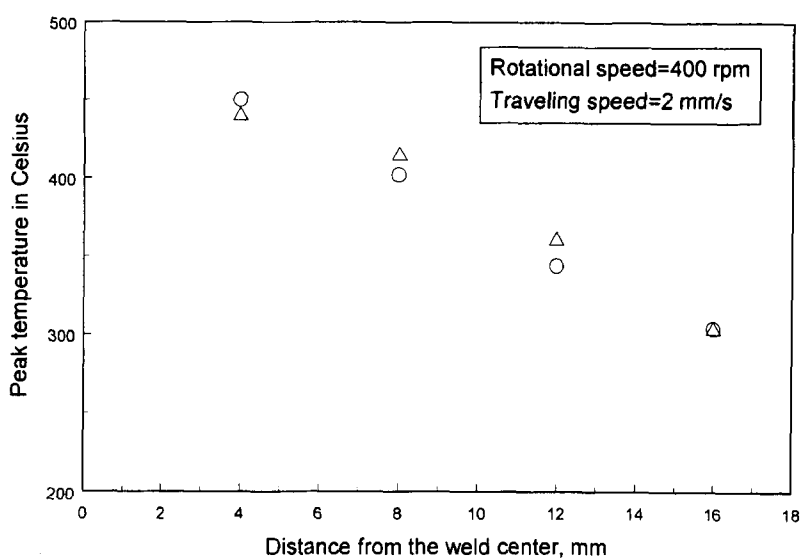


Figure 7. Maximum temperature for thermocouples located at equal distances but on opposite sides of weld seam.

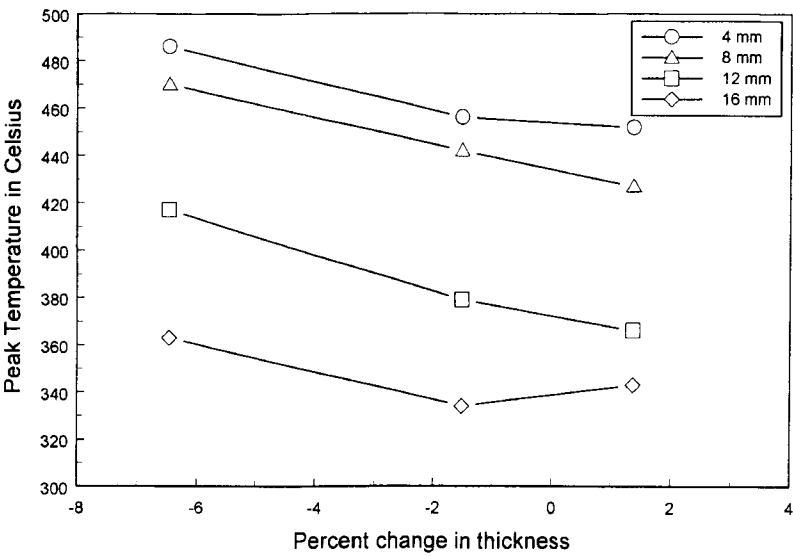


Figure 8. Effect of pin tool pressure on maximum temperature. Note that with the greatest reduction in specimen thickness (maximum pressure) the temperature increases modestly.

manually, so it was not possible to obtain exactly the same pressure for each weld. The change of the welded seam thickness compared with the parent aluminum is a measure of the welding pressure when other parameters are the same. Figure 8 shows the peak temperature distribution of welded joints with different thickness changes and correspondingly different pressures after welding at a rotational speed of 1200 rpm. It is clear that higher temperature of the welded joint is caused by the higher welding pressure, but the temperature always remains below the melting temperature of the aluminum. Note that at the lowest pressure used, the weld was actually thicker than the parent aluminum because a tunnel formed near the bottom of the weld.

INFLUENCE OF ROTATIONAL SPEED ON THE TEMPERATURE FIELD

In the welding process, the heat may come from friction between the workpiece and the pin

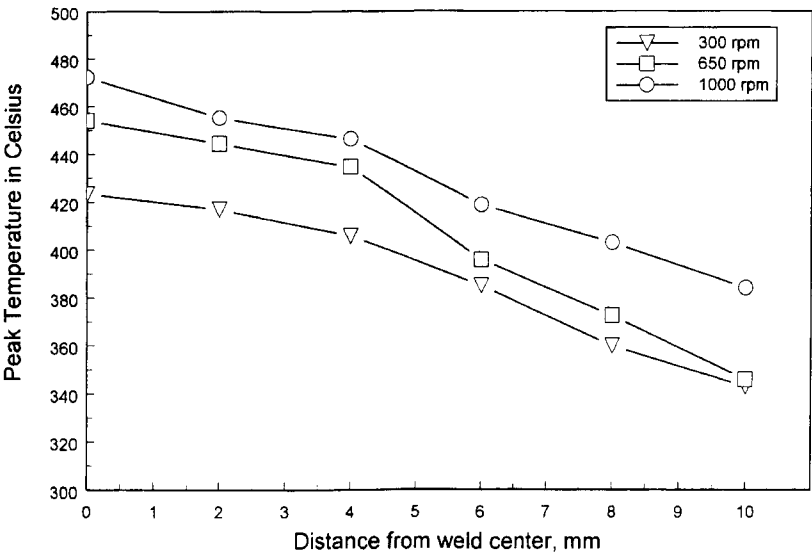


Figure 9. Influence of rotational speed on maximum temperature. Temperature was measured at the midpoint of the sample thickness.

TABLE 1. 6061-T6 Yield Strength at Different Temperatures [11].

Temperature (°C)	Yield Strength (Ksi)	Yield Strength (MPa)
24	40	280
100	38	270
149	31	220
204	15	105
260	5	35
315	2.7	20
371	1.8	15

tool as well as from plastic deformation of the workpiece. The rotational speed of the pin tool may change each of these. The influence of the pin tool rotational speed on the temperature field is shown in Figure 9. From Figure 9, it is clear that the rotational speed has only a modest effect on the peak temperature. Within the weld zone the peak temperature increased almost 40°C when the rotational speed increased from 300 rpm to 650 rpm, but the peak temperature increases only 20°C more when the rotational speed increased from 650 rpm to 1000 rpm. With a higher rotational speed, the temperature should increase, but increased temperature reduces the metal flow stress and the torque which limits any power generation increase. The yield strength of 6061-T6 at different temperatures is shown in Table 1 [11]. The actual strength of the aluminum may be somewhat higher than indicated in Table 1 since the workpiece only sees the temperature for a few seconds. Overaging, however, seems to take place very quickly since preliminary measurements in this laboratory indicate that only very modest translational forces are needed to advance the pin tool. Nevertheless, with higher temperatures the normal force between pin tool and the workpiece may relax as the material becomes hotter, thereby reducing friction force and power generation due to relative slippage.

EFFECT OF THE PIN TOOL SHOULDER

In these experiments the diameter of the shoulder was twice that of the nib. The effect of the

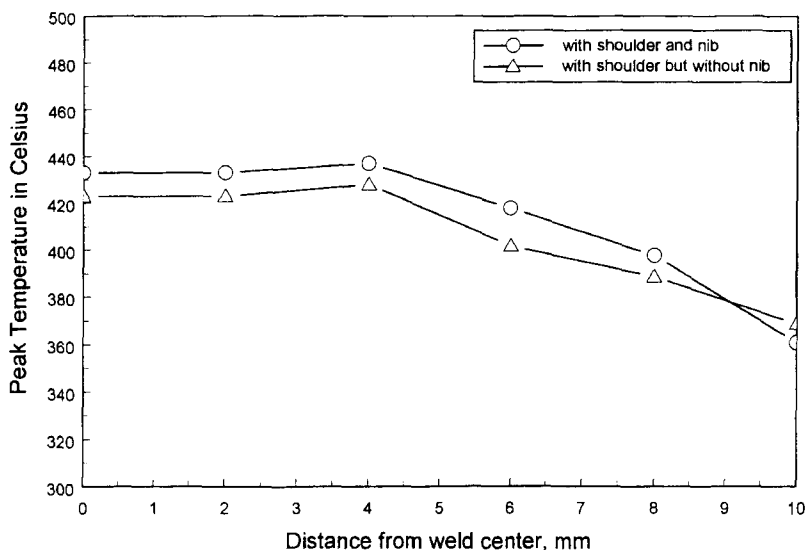


Figure 10. Maximum temperature for welds made with and without the nib. Note that shoulder contributes most of heat. Weld was made at 400 rpm and 2 mm/sec travel speeds.

shoulder in the welding process is to generate heat through deformation of metal, to prevent the metal from exiting the welded seam during welding and to clean the specimen surface by pushing aside the aluminum oxide film on the specimen surface. Figure 10 shows the peak temperature at various distances from the weld center with and without the nib. It is seen that the shoulder dominates the pattern of flow deformation and heat generation in the metal. This is expected since the area of the shoulder is greater than the area of the nib in contact with the workpiece, the vertical force between the shoulder and the workpiece is greater than the force between the nib and the workpiece (more detailed measurements of these forces is underway) and the shoulder has a higher linear velocity than the smaller radius nib.

CONCLUSIONS

1. Under the conditions used in these experiments, the welding temperature is no more than $0.8T_m$. Porosity and hot cracking, which can occur in aluminum fusion welding, are avoided because of the solid state welding process.
2. The grains of the weld center are fine and equiaxed because of the stirring and high deformation which facilitates dynamic recrystallization. Mechanical properties and fracture toughness should be improved by this structure.
3. For a given set of welding conditions, the maximum temperature of the weld zone is nearly constant throughout the center region of the weld.
4. Higher welding pressures cause higher welding temperatures. However, the temperature never exceeds the melting temperature.
5. Increasing rotational speed of the pin tool increases the welding temperature, but the incremental effect decreases with increasing rotational speed.
6. The shoulder dominates the friction stir welding process in the geometry investigated. It controls the flow field and heat generation, prevents metal extrusion, and cleans the specimen surface.

ACKNOWLEDGEMENTS

The authors would like to acknowledge the generous support of NASA Marshall Space Flight Center under grant number NCC8-137. David Brown at UTEP gave much valuable assistance in experimental work.

REFERENCES

1. W. M. Thomas et al. 1991. "Friction Stir Butt Welding." International Patent Application No. PCT/GB92/02203 and GB Patent Application No. 9123978.8.
2. H. B. Cary. *Modern Welding Technology*. Prentice Hall, New Jersey.
3. C. J. Dawes and W. M. Thomas. 1996. "Friction Stir Process Welds Aluminum Alloys." *Welding Journal*, pp. 41–45, March.
4. C. J. Dawes. 1995. "An Introduction to Friction Stir Welding and Its Development." *Welding & Metal Fabrication*, pp. 13–16, January.
5. G. Liu, L. E. Murr, C. S. Niou, J. C. McClure and F. R. Vega. 1997. "Microstructural Aspects of the Friction-Stir Welding of 6061-T6 Aluminum." *Scripta Materiala*, Vol. 37, No. 3, pp. 355–361.
6. O. T. Midling. 1994. "Material Flow Behavior and Microstructural Integrity of Friction Stir Butt Weldments." *Proceedings of 4th International Conference on Aluminum Alloys*, Atlanta, GA.
7. L. E. Murr, R. D. Flores, O. V. Flores, J. C. McClure, G. Liu and D. Brown. 1998. "Friction-Stir Welding: Microstructural Characterization." *Mat. Res. Innovat.*, No. 1, pp. 211–223.
8. L. E. Murr, G. Liu and J. C. McClure. 1998. "A TEM Study of Precipitation and Related Microstructures in Friction-Stir Welded 6061 Aluminum." *Journal of Materials Science*, Vol. 33, pp. 1243–1251.
9. J. C. McClure, Z. Feng, W. Tang, J. E. Gould, L. E. Murr and X. Guo. 1998. "A Thermal Model of Friction Stir Welding." *Proceedings 5th International Conference on Trends in Welding Research*, Pine Mountain, Georgia, June.
10. J. R. Davis. 1994. *ASM Specialty Handbook—Aluminum and Aluminum Alloys*, ASM International.
11. *Handbook of Aluminum*, Alcan Aluminum Corporation, 1970.